Science of the Total Environment 916 (2024) 170044

Contents lists available at ScienceDirect

Science of the Total Environment

journal homepage: www.elsevier.com/locate/scitotenv

The role of marine fish-produced carbonates in the oceanic carbon cycle is determined by size, specific gravity, and dissolution rate

Erik J. Folkerts [a,*], Amanda M. Oehlert [b], Rachael M. Heuer [a], Sandy Nixon [a], John D. Stieglitz [a], Martin Grosell [a]

[a] Department of Marine Biology and Ecology, Rosenstiel School of Marine, Atmospheric, and Earth Science, University of Miami, Miami, FL 33149, United States of America
[b] Department of Marine Geosciences, Rosenstiel School of Marine, Atmospheric, and Earth Science, University of Miami, Miami, FL 33149, United States of America

HIGHLIGHTS

- Fate of marine fish-produced carbonates (ichthyocarbonates) investigated.
- Novel ichthyocarbonate physical and chemical metrics measured to model fate.
- Abundant ichthyocarbonate dissolution before euphotic zone clearance (~200 m).
- Larger ichthyocarbonate can sink to depths below 1000 m.
- Significant ichthyocarbonate dissolution in shallow, supersaturated environments.

GRAPHICAL ABSTRACT

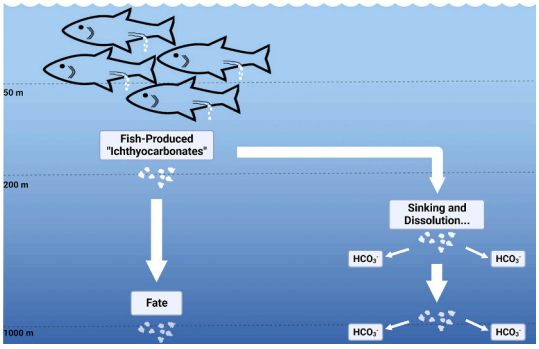

ARTICLE INFO

Editor: Jay Gan

Keywords:
Carbon cycle
Marine teleosts
Ichthyocarbonates
Alkalinity budget

ABSTRACT

Rising CO_2 emissions have heightened the necessity for increased understanding of Earth's carbon cycle to predict future climates. The involvement of marine planktonic species in the global carbon cycle has been extensively studied, but contributions by marine fish remain poorly characterized. Marine teleost fishes produce carbonate minerals ('ichthyocarbonates') within the lumen of their intestines which are excreted at significant rates on a global scale. However, we have limited understanding of the fate of excreted ichthyocarbonate. We analyzed ichthyocarbonate produced by three different marine teleosts for mol%$MgCO_3$ content, size, specific gravity, and dissolution rate to gain a better understanding of ichthyocarbonate fate. Based on the species examined here, we report that 75 % of ichthyocarbonates are ≤0.91 mm in diameter. Analyses indicate high Mg^{2+} content across species (22.3 to 32.3 % mol%$MgCO_3$), consistent with previous findings. Furthermore, ichthyocarbonate specific gravity ranged from 1.23 to 1.33 g/cm^3, and ichthyocarbonate dissolution rates varied among species as a function of aragonite saturation state. Ichthyocarbonate sinking rates and dissolution depth were estimated for the Atlantic, Pacific, and Indian ocean basins for the three species examined. In the North Atlantic, for example, ~33 % of examined ichthyocarbonates are expected to reach depths exceeding 200 m prior to complete dissolution. The remaining ~66 % of ichthyocarbonate is estimated to dissolve and contribute to shallow water alkalinity budgets. Considering fish biomass and ichthyocarbonate production rates, our results

* Corresponding author at: Department of Biological Sciences, University of Manitoba, Winnipeg, MB R3T 2N2, Canada.
E-mail address: efolkert@ualberta.ca (E.J. Folkerts).

https://doi.org/10.1016/j.scitotenv.2024.170044
Received 22 October 2023; Received in revised form 5 January 2024; Accepted 7 January 2024
Available online 18 January 2024

support that marine fishes are critical to the global carbon cycle, contributing to oceanic alkalinity budgets and thereby influencing the ability of the oceans to neutralize atmospheric CO_2.

1. Introduction

Given the increasing levels of carbon dioxide (CO_2) emissions worldwide, determining how the global carbon cycle responds to increased concentrations of atmospheric CO_2 is imperative for understanding future climate scenarios. Two primary processes comprise the movement of oceanic carbon: the biological pump and the marine inorganic carbon cycle. The biological pump refers to the downward flux of organic carbon produced in the surface ocean to depths below the euphotic zone, where it is respired or consumed by organisms (including mesopelagic bacteria, zooplankton, and fishes), or settles on the bottom of the ocean (organism deadfall or deposition) (Saba et al., 2021; Sarmiento et al., 1995; Honjo et al., 2014; Buesseler et al., 2020; Nowicki et al., 2022). The marine inorganic carbon cycle comprises an integrated process where atmospheric carbon (as CO_2) is continually exchanged with carbon from oceanic surface water, the deep ocean, and sedimentary environments (Millero, 2005). Factoring into this cycle are the biomineralization processes of many marine organisms which combine dissolved bicarbonate (HCO_3^-) ions in seawater with calcium (Ca^{2+}) ions to precipitate insoluble calcium carbonate ($CaCO_3$) to form their shells or skeletons described by the following overall reactions (Millero, 2007):

$$CO_{2(aq)} + H_2O \leftrightarrow H^+ + HCO_3^-$$

$$Ca^{2+} + 2HCO_3^- \leftrightarrow CaCO_3 + CO_2 + H_2O$$

Traditionally, planktonic organisms are viewed as responsible for the majority of marine $CaCO_3$ production, with coccolithophores (phylum Haptophyta) and Foraminifera being the two primary unicellular phyletic groups (Feely et al., 2004; Schiebel, 2002) each producing an estimated 1–1.2 Pg $CaCO_3$-C yr^{-1} (Broecker, 2009; Langer, 2008) of the 0.5–2.0 $CaCO_3$-C yr^{-1} produced in surface oceans (Iglesias-Rodriguez et al., 2002; Milliman and Droxler, 1996) - although modern modelling efforts suggest pteropods may also produce volumetrically significant quantities of aragonite (Buitenhuis et al., 2019). Once dead, carbonate shells from these organisms sink to deeper ocean depths, where ambient conditions facilitate either dissolution or deposition into sedimentary environments. Dissolution releases HCO_3^- at these deeper depths and contributes to overall oceanic alkalinity budgets (Ducklow et al., 2001). In contrast, carbonate sediments that are deposited on the seafloor impact the global carbon cycle differently depending on the time scale considered. In the short-term carbon cycle (<1000 years), the formation of carbonate minerals from seawater is known to result in a net flux of CO_2 back to the atmosphere (Frankignoulle et al., 1994, 1995; Gattuso et al., 1993; Ware et al., 1992), while in the long-term carbon cycle (millennia and longer), carbonate deposition in the oceans can act as a sink for inorganic carbon (Ducklow et al., 2001; Passow and Carlson, 2012).

Complementing these contributions by calcifying planktonic species, marine teleost fish are increasingly being recognized as important contributors to the carbonate pump (Bianchi et al., 2021; Saba et al., 2021; Wilson et al., 2009; Woosley et al., 2012). Marine teleost fish species produce carbonate precipitates (termed "ichthyocarbonates") as part of their osmoregulatory strategy and these ichthyocarbonates are continuously excreted and released into their surrounding environments (Grosell, 2006; Grosell and Oehlert, 2023; Walsh et al., 1991; Wilson et al., 2002). Fish in marine environments are challenged osmotically due to higher seawater osmotic pressures (~ 1000 mOsmol) versus organism internal conditions (~ 330 mOsmol). This osmotic gradient results in marine fish water loss and ion gain (Evans et al., 2005). To counteract this, marine fish excrete ions at the gills and ingest large volumes of seawater to maintain hydration (Evans et al., 2005; Grosell and Taylor, 2007; Marshall and Grosell, 2005). Within the intestinal tract, imbibed seawater is alkalinized (pH 8.5–9.2) from tissue HCO_3^- secretion, with gut fluid measurements ranging from 50 to 100 mM HCO_3^- compared to seawater HCO_3^- concentrations ~2.2 mM (McDonald and Grosell, 2006; Wilson et al., 1996, 2002). Intestinal water absorption in marine fish was thought to solely occur as a result of Na^+ and Cl^- uptake across the epithelia (powered primarily through enterocyte $Na^+ - K^+$ ATPase pump activity) (Grosell and Taylor, 2007; Marshall and Grosell, 2005). However, an additional and crucial component of this process has more recently been discovered which further contributes to water absorption and fish survival in marine environments (Grosell, 2006). As imbibed divalent rich seawater is alkalinized by the gut epithelia, Ca^{2+} and Mg^{2+} combine with CO_3^{2-} to form Mg-rich $CaCO_3$ precipitates (ichthyocarbonates) which are ultimately excreted into the environment. As a consequence of ichthyocarbonate formation, it is estimated that luminal osmotic pressures in marine fish are reduced by >100 mOsmol. This reduction produces favorable osmotic gradients between the gut lumen and enterocytes/body fluids of marine fish which allow for essential water absorption across the intestine (Grosell, 2011; Grosell et al., 2009; Grosell and Oehlert, 2023; Whittamore et al., 2010; Wilson et al., 2002).

Marine teleost ichthyocarbonate production was first estimated to be responsible for approximately 0.04 to 0.11 Pg of $CaCO_3$-C yr^{-1} or 2.7–15.4 % of total new $CaCO_3$ production in surface oceans each year (although more liberal modelling assumptions concluded it could be as high as 45 %; Wilson et al., 2009). However, while one study reports that these values might be an overestimation (Ghilardi et al., 2023), recent global fish biomass estimates (Bianchi et al., 2021) higher than the values used by Wilson et al. (2009) suggest that potentially ~5-fold higher ichthyocarbonate production may occur in global oceans, indicating an even more important role in the marine carbonate budget than previously anticipated. Although research on the production of ichthyocarbonate is growing, the fate of ichthyocarbonates upon excretion is understudied and relatively unknown. Determining the contributing factors to oceanic alkalinity budgets and properties of ocean carbonate chemistry with depth is an important endeavour since the flux of carbon from surface to deep ocean environments is a major process in the global carbon cycle. The global carbon cycle profoundly impacts Earth's climate, oceanic biogeochemical properties, and overall marine ecosystem viability and productivity (Ducklow et al., 2001; Siegel et al., 2016; Volk and Hoffert, 2013). The dissolution of carbonate minerals and the production of alkalinity in the oceans are particularly important to quantify because deep ocean CO_3^{2-} concentrations govern the oceans' response to changing atmospheric CO_2 concentrations over millennial timescales (Berner, 2001; Ridgwell and Zeebe, 2005; Zeebe, 2012). Thus, quantitative understanding of carbonate mineral dissolution depths is critical in the determination of the impact of anthropogenic CO_2 emissions on marine settings (Doney et al., 2009; Feely et al., 2004; Orr et al., 2005).

The role of ichthyocarbonate in oceanic alkalinity budgets has previously been attributed to their high solubility (Wilson et al., 2009; Woosley et al., 2012). Potentially owing to their high Mg^{2+} content (Foran et al., 2013; Perry et al., 2011; Salter et al., 2017, 2018, 2019; Walsh et al., 1991; Wilson et al., 2009; Woosley et al., 2012), ichthyocarbonate dissolution has been proposed to contribute alkalinity to the marine inorganic carbon cycle and possibly be responsible for elevated normalized total alkalinity observations above aragonite saturation horizons (Wilson et al., 2009; Woosley et al., 2012), although a recent study of north Pacific carbonate chemistry concluded otherwise (Subhas et al., 2022). Recent work supports the presence of an active carbonate

cycle in the shallow oceans (Adkins et al., 2021; Carter et al., 2021; Dong et al., 2018; Subhas et al., 2022; Sulpis et al., 2021), a phenomenon called upon to explain the imbalance between surface ocean carbonate production and accumulation in the deep sea (Milliman, 1993). Dissolution of biogenic carbonate minerals such as those produced by pteropods (Buitenhuis et al., 2019) and marine fish (Wilson et al., 2009; Woosley et al., 2012) have been inferred to drive a portion of this shallow carbonate cycle. However, critical knowledge gaps regarding the production magnitude, dissolution rate, and ultimately the fate of these biogenic carbonates remain. Indeed, in sedimentary environments at shallower depths, ichthyocarbonates are estimated to comprise 14–70 % of fine fraction sediment in tropical marine settings (Perry et al., 2011), while also being a major contributor to shallow ocean alkalinity budgets (Martin et al., 2021; Woosley et al., 2012). Clearly further research is needed to understand and characterize ichthyocarbonate fate within oceanic environments to better delineate how fish contribute to the global carbon cycle.

In the current study, dissolution and sinking rates of ichthyocarbonates produced by three different species of marine fish occupying differing marine ecological niches were determined to provide estimates of ichthyocarbonate fate within oceanic water columns. Our results indicate that ichthyocarbonate size, along with specific gravity, heavily influences sinking rate. Furthermore, ichthyocarbonate dissolution is significantly affected by seawater aragonite saturation state (Ω_{arag}), with ichthyocarbonate produced by some fish species predicted to reach depths beyond 1000 m. Collectively, we demonstrate that ichthyocarbonate is likely an important contributor to both shallow ocean carbonate cycles and the distribution of ocean alkalinity through space and time.

2. Materials and methods

2.1. Experimental organisms and Ichthyocarbonate collections

Gulf toadfish (*Opsanus beta*) used for ichthyocarbonate collections were from a population housed at the Rosenstiel School of Marine, Atmospheric and Earth Science, University of Miami (Miami, FL, USA). Four age-specific groups were used and analyzed: "yearlings" = 6.31 ± 5.41 g, two juvenile groups = 61.6 ± 42.7 g and 77.3 ± 32.5 g, and adults = 207.3 ± 57.7 g. Fish were housed in 30 L glass tanks supplied with continuous aeration and flow-through, sand-filtered, Biscayne Bay seawater (33–35 ppt, 25 °C). Depending on sizes, groups of 2–15 fish were housed per tank. Fish were fed to satiation weekly with squid. Ichthyocarbonates from each Gulf toadfish age class were collected from tank bottoms using plastic transfer pipettes. Once enough ichthyocarbonates were collected, fecal matter and other debris (fish scales, uneaten food, etc.) were removed and ichthyocarbonates were then washed briefly three times in MilliQ double distilled pure water prior to analyses. Toadfish care, husbandry, and ichthyocarbonate collections were performed according to approved University of Miami Animal Care protocols (Institutional Animal Care and Use Committee No. 22–150 LF).

Juvenile olive flounder (*Paralichthys olivaceus*, 202.0 ± 1.5 g) and juvenile yellowtail snapper (*Ocyurus chrysurus*, 21.0 ± 3.7 g) spawned from broodstock were housed and maintained in 15,000 L fiberglass holding tanks at the University of Miami's Experimental Hatchery (UMEH) using similar spawning and rearing techniques to those described previously for these species at UMEH (Stieglitz et al., 2021, 2022). Tanks were supplied with flow-through, filtered seawater from the adjacent Atlantic Ocean and constant aeration (33–35 ppt, 18 °C and 33–35 ppt, 25 °C for flounder and yellowtail snapper, respectively). Juvenile flounder and yellowtail snapper were fed daily to satiation with a standard commercial grower pelletized diet (Europa Marine Grower Diet, Skretting, Tooele, UT, USA). To collect ichthyocarbonates from flounder, which comprised a portion of the settleable solids in holding tank effluent water, the waste drain valves were opened and purged waste containing the carbonates was collected into 20 L buckets. When collecting from yellowtail snapper tanks, ichthyocarbonates were siphoned into 20 L buckets. Once in collecting buckets, both yellowtail snapper and flounder ichthyocarbonates were collected by plastic transfer pipettes and briefly washed three times with MilliQ double distilled water to remove fecal matter, salt, and other debris. For all species of fish (toadfish, flounder, yellowtail snapper), special care was made during collection to exclude any non-carbonate components, including fecal matter or undigested food. Flounder and yellowtail snapper rearing and husbandry over the course of this study were performed according to approved University of Miami Animal Care protocols (Institutional Animal Care and Use Committee No. 20–138). All chemicals used in the current study were purchased from MilliporeSigma (MA, USA) unless otherwise stated.

2.2. Measurement of ichthyocarbonate diameter and size distribution

Ichthyocarbonates produced by all species of fish were transferred to a shallow glass petri dish, viewed under a Nikon SMZ800N stereomicroscope (Nikon, Japan), and images were recorded with a digital camera. ImageJ software (v1.53e, NIH, USA) was then used to measure and record ichthyocarbonate dimensions, including diameter and total surface area. A nonlinear, 2-parameter power regression ($f = a * x^b$) was applied to diameter measurements of ichthyocarbonates from the four size-classes of toadfish using Sigmaplot software (v13.0, Systat Software Inc., USA) to relate fish mass to ichthyocarbonate diameter. Yellowtail snapper and olive flounder single size-class ichthyocarbonate diameters were then plotted on the derived function to validate relationships. Total number (n) of ichthyocarbonate measurements made for each species were 74, 109, 110, 158, 51, and 155 for adult toadfish, the juvenile toadfish groups, sub-juvenile toadfish, yearling toadfish, juvenile flounder, and juvenile yellowtail snapper, respectively.

2.3. Ichthyocarbonate Mg^{2+} and Ca^{2+} measurement

Ichthyocarbonate Mg^{2+} and Ca^{2+} concentrations were analyzed via flame atomic absorption spectrometry (AAS) using a 220 FS SpectrAA atomic absorption spectrometer (Varian Inc., CA, USA). Following collection and washes (see above), ichthyocarbonates were dried overnight at 37 °C, weighed, and subsequently dissolved in known volumes of trace metal grade nitric acid. Samples were then diluted for AAS analyses in a 0.1 % lanthanum chloride solution to bring samples into range of freshly made, matrix-matched standards for concentration analysis. Results are reported as mol%$MgCO_3$ under the assumption that all Mg^{2+} and Ca^{2+} were present as $MgCO_3$ and $CaCO_3$, as previously reported (Salter et al., 2019).

2.4. Ichthyocarbonate and coral skeleton dissolution measurements

To measure dissolution rates, known weights of ichthyocarbonates from each species (pooled carbonates across age classes for toadfish) were first placed into aeration chambers (modified 50 mL conical tubes with cap holes to introduce polyethylene tubing aeration lines) filled with 15 mL of ambient temperature, UV-sterilized, 1.0 μm filtered seawater. Chambers were then supplied with continuous gentle aeration to induce ichthyocarbonate movement within the chamber for dissolution periods of 1.5–4 h. Control samples of seawater were treated similarly for matching periods of time. Following the dissolution period, 10 mL of aeration chamber solutions were extracted, centrifuged briefly (< 30 s), and transferred to titration chambers for double endpoint total titratable alkalinity measurements as described previously (Brix et al., 2013).

Briefly, initial pH measurements were recorded for all aerated samples prior to analyses. Double endpoint total titratable alkalinity was determined by first gassing 10 mL solutions with N_2 for 15 min. Subsequent pH was recorded and known volumes of 0.2 N HCl were added

to 10 mL samples using 200 μL-volume microburettes (Gilmont Instruments, USA) under continues N_2 gassing until pH = 3.8 was achieved. Samples were held at pH = 3.8 for 15 min. Following this period, volumes of 0.02 N NaOH were added back to solutions using microburettes to return pH to the starting value under continued N_2 gassing. Total mols of titratable alkalinity were calculated as the difference between the mols of H^+ added (HCl titration) and mols of OH^- (NaOH titration). Rates of ichthyocarbonate dissolution were then calculated as: $d/dt_{dissolution} = ((M_i - M_{sw}) \cdot v) / (m \cdot t)$), where M_i is mM of titratable alkalinity in ichthyocarbonate samples, M_{sw} is mM of titratable alkalinity in matching seawater control samples, v is the volume of original solutions in aeration chambers (15 mL), m is the mass of ichthyocarbonates placed into aeration chambers, and t is the duration of dissolution. Rates of ichthyocarbonate dissolution are expressed as μmol eqv g^{-1} h^{-1}. Dissolution rates were plotted against Ω_{arag} for each respective titration. CO_2sys (Lewis et al., 2006) was used to calculate Ω_{arag} at the onset and end of each dissolution rate measurement using a salinity of 36 ppt, temperature of 25 °C, and measurements of pH and total alkalinity at the onset and end of each dissolution rate measurement. Parameterization was conducted in the same way as previously described (Woosley et al., 2012), with the exception that K_1 and K_2 CO_2 constants were parameterized using Mehrbach and colleagues' (Mehrbach et al., 1973) constants refit by Lee and associates (Lee et al., 2000). Number of performed ichthyocarbonate dissolutions measurements (n) were 52, 48, and 31 for toadfish, flounder, and yellowtail snapper, respectively. Dissolution rates for each species were plotted as a function of the geometric mean of Ω_{arag} at the onset and end of each measurement and 2-parameter exponential decay non-linear regressions ($f = a * exp(-b * x)$) were performed for each species. For comparative purposes, known masses of crushed coral skeletons (*Acropora* sp.) were also treated to the above protocols to determine rates of coral skeleton dissolution. These coral values highlight the differences between ichthyocarbonate – and therefore high magnesium calcite (HMC) – dissolution versus that of aragonite produced by more classically considered marine calcifiers.

2.5. Ichthyocarbonate dissolution rate measurement via pH-stat validation

To validate dissolution protocols discussed above, seven dissolution rate measurements of Gulf toadfish ichthyocarbonate were performed via pH-Stat. Briefly, following collection and rinsing procedures listed in Section 2.4, ichthyocarbonates were loaded into titrating vessels filled with ambient temperature UV-filtered seawater supplied with constant aeration. Individual vessels were also outfitted with a pH electrode and a 0.2 N HCl supply line. After initial pH recordings were made, ichthyocarbonates were allowed to dissolve over 2 h, with small increments of HCl added to titrating vessels (using microburettes) to maintain pH at initially recorded levels. Time, accumulated volume of HCl added, and pH were recorded every minute. At the end of titration periods, slopes of HCO_3^- release and increased alkalinity (measured via amounts of HCl added) were calculated and converted to μeqv g^{-1} h^{-1} and compared against toadfish ichthyocarbonate dissolution rates measured via double endpoint protocols described in Section 2.4.

2.6. Ichthyocarbonate specific gravity measurements

Ichthyocarbonate specific gravity was measured using methods previously established for determining specific gravity of fish embryos in the field (Pasparakis et al., 2022). Briefly, a series of 12 beakers containing solutions ranging in densities from 1.160 to 1.400 g/mL were made by mixing pre-calculated volumes of ethanol and tetrachloroethylene (VWR, USA and Macron Fine Chemicals, Avantor, USA, respectively). Densities were verified by a DMA 35 specific gravity meter (Anton Paar, Graz, Austria). Per each density solution, five ichthyocarbonates were placed into respective beakers using a glass transfer pipette and gently mixed (to ensure solution surface tensions did not cause ichthyocarbonates to initially rest on top of solutions). Following a 2-min settling period, ichthyocarbonate buoyancies were scored either as "1" (floating at the surface), "0" (suspended in solution), or "-1" (resting on the bottom). Average buoyancies for species specific ichthyocarbonates were then plotted against solution specific densities and a nonlinear regression 4-parameter sigmoidal equation ($f = y0 + a / (1 + exp(-(x - x0) / b))$) was applied using Sigmaplot software (v13.0, Systat Software Inc., USA), where $x0$ = the neutral buoyancy of the ichthyocarbonates. For regression analyses, r^2 values ranged from 0.995 to 0.998 for the three fish species calculated specific gravity curves. For toadfish measurements, ichthyocarbonates from all four previously defined distinct age classes were pooled together for analyses. Total number (n) of ichthyocarbonates produced by each species measured for specific gravity ranged from 30 to 45.

2.7. Ichthyocarbonate depths of dissolution and fate modelling

Two of the three species examined here are benthic and the third is a reef fish. As such the ichthyocarbonates produced by these species will be released at or near the sea floor at shallow depths. However, in the following we assume that the examined ichthyocarbonates represent marine teleost fish in general and therefore are useful to estimate fate of ichthyocarbonates excreted by all species, including open ocean fishes. Further, we assume that ichthyocarbonates in general are excreted near the ocean surface. Ichthyocarbonate sinking rates were calculated from specific gravity and size using the buoyant velocity integrated approach (Zheng and Yapa, 2000) assuming spherical shapes and seawater specific gravity of 1.030 g ml^{-1} at 20 °C. Selected ichthyocarbonate sizes were chosen following a published generalized distribution of global fish biomass across a suite of fish size ranges (Jennings et al., 2008) and then calculated median fish size in grams for each of the size classes reported. The predicted diameter of ichthyocarbonate pellets was calculated based on these median fish sizes using the equation: $d = 0.836*(m^{0.162})$, where d is ichthyocarbonate diameter in mm and m is fish mass in g. The coefficients 0.836 and 0.162 are derived from nonlinear regressions outlined in Section 2.2. Predicted ichthyocarbonate diameters were then classified under the Udden-Wentworth particle size classification

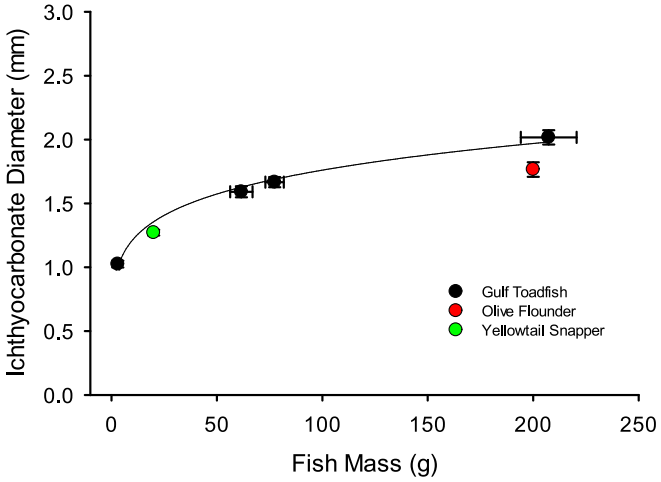

Fig. 1. Ichthyocarbonate diameter as a function of fish mass. Using differing life stages/sizes of Gulf toadfish (*Opsanus beta*), a nonlinear 4-parameter sigmoidal regression was applied to relate fish mass to ichthyocarbonate diameter. Two other marine fish species, yellowtail snapper (*Ocyurus chrysurus*) and olive flounder *(Paralichthys olivaceus)* of one size class each are included. Total number (n) of ichthyocarbonate size measurements made were 74, 109, 110, 158, 51, and 155 for adult toadfish, two juvenile stages of toadfish, yearling toadfish, juvenile flounder, and juvenile yellowtail snapper, respectively. Data are presented as mean ± standard error.

Table 1
Ichthyocarbonate Mg^{2+} content from three different species of marine fish. Ichthyocarbonates were analyzed via flame atomic absorption spectrometry. All data are presented as mean ± standard error ($n = 5$).*

Species	Mol% $MgCO_3$
Gulf toadfish (*Opsanus beta*)	32.3 ± 0.8[a]
Olive flounder (*Paralichthys olivaceus*)	24.5 ± 0.2[a,b]
Yellowtail snapper (*Ocyurus chrysurus*)	22.3 ± 0.8[b]

* Superscript letters denote significant differences between determined species values ($p < 0.05$).

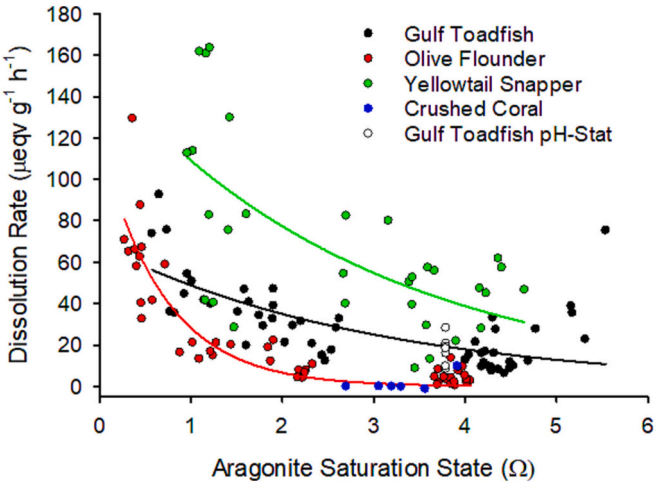

Fig. 2. Ichthyocarbonate dissolution rate versus aragonite saturation state. Samples (~ 100 mg) of ichthyocarbonates from three marine teleosts (and ground coral) were allowed to dissolve in filtered seawater and the resulting alkalinity release titrated to determine dissolution rate relative to aragonite saturation state (geometric mean of initial and final aragonite saturation state calculated using CO_2sys for each dissolution measurement). Number of performed ichthyocarbonate dissolutions measurements (n) were 52, 48, 31, 6, and 7 for Gulf Toadfish (*Opsanus beta*), Olive Flounder (*Paralichthys olivaceus*), Yellowtail Snapper (*Ocyurus chrysurus*), coral, and Gulf Toadfish pH-Stat, respectively.

scheme (Wentworth, 1922). Fractions of total fish ichthyocarbonate production were summed for size classes. From the sinking rates, depth at which the ichthyocarbonate occurs at a given time after excretion was calculated and related to Ω_{arag} and temperature depth profiles from the Atlantic, Pacific and Indian Oceans using mean values from 10° N to 30° N latitude for all basins (Jiang et al., 2015). From the determined relationships between Ω_{arag} and dissolution rate, dissolution rates were calculated as a function of time after excretion at the surface ocean (and thereby the depth to which they have sunk). The influence of dissolution rates on ichthyocarbonate size over time was taken into account for determination of sinking rates. Similarly, the influence of temperature on seawater viscosity was considered. From these calculations, the depth of full dissolution of ichthyocarbonates were determined. Note that while the direct effect of Ω_{arag} on dissolution rates and dissolution depths was encompassed in these estimates, the influence of temperature on the dissolution depths includes only the effects on seawater viscosity and therefore sinking rates, and not the potential effect of temperature or pressure on dissolution rates.

2.8. Statistics and data analysis

All data were assessed for normality and equal variance via Shapiro-Wilk and Brown-Forsythe tests, respectively, when statistical tests were performed. For statistical analyses, plotting metrics, and nonlinear curve-fitting procedures, SigmaPlot v.13.0 (Systat Software Inc., USA) or Prism v. 6.02 (GraphPad Software Inc., USA) was used. For ichthyocarbonate Mg^{2+} compositional analyses, a one-way ANOVA on ranks was performed, while for dissolution rate versus aragonite comparisons, a two-way ANOVA was performed. Following ANOVA analyses, Holm-Sidak *post-hoc* multiple comparison tests were used to determine significant differences among fish species. For nonlinear regression comparisons, unpaired *t*-tests with pairwise correction factors were used to determine statistical differences among respective regression coefficients between species. $p < 0.05$ was used as the fiducial level of significance. All data are presented as mean ± standard error of the mean (SEM).

3. Results

3.1. Ichthyocarbonate morphometrics and elemental composition

Toadfish ichthyocarbonate diameter correlated with fish mass across four size classes and ichthyocarbonate produced by flounder and yellowtail snapper (from a single, respective size range of fish in each species) fell in-line with the relationship observed for toadfish (Fig. 1). Ichthyocarbonate ranged in diameter from 0.41 to 3.70 mm across all species investigated, ranging from medium sand to gravel in the Wentworth size classification scheme. Ichthyocarbonate produced by the three species of fish investigated had significantly different mol% $MgCO_3$ concentrations. Ichthyocarbonate mol% $MgCO_3$ values were determined to be 32.3 %, 24.5 %, and 22.3 % for toadfish, flounder, and yellowtail snapper, respectively (Table 1).

3.2. Rates of ichthyocarbonate dissolution and buoyancy

Dissolution rate of ichthyocarbonates assessed via double endpoint titrations across various Ω_{arag} revealed a general inverse relationship (Fig. 2). Overall, yellowtail snapper ichthyocarbonate dissolution rates were highest, while flounder ichthyocarbonates exhibited the lowest dissolution rates across Ω_{arag} (Fig. 2). However, non-linear regression analyses revealed unique differences in ichthyocarbonate dissolution rates among species across Ω_{arag} (Fig. 2, Table 2). For example, at $\Omega_{arag} = 1$, ichthyocarbonate produced by yellowtail snapper dissolves ~4× faster than that produced by the olive flounder, while at higher saturations states, the difference in dissolution rates becomes more pronounced (e.g., at $\Omega_{arag} = 4$, yellowtail snapper ichthyocarbonate dissolves ~108× faster than that of olive flounder; Fig. 2, Table 3). Ichthyocarbonate also dissolved much more readily than crushed coral, while toadfish ichthyocarbonate dissolution rates measured via pH-Stat methods were equitable with measurements made via double end-point

Table 2
Coefficient comparisons for ichthyocarbonate dissolution rate and specific gravity non-linear regression analyses. Values are depicted as x ± standard error.*

	Dissolution $f = a*exp(-b*x)$		Specific gravity $f = y0 + a/(1 + exp(-(x-x0)/b))$
Species	Coefficient *a*	Coefficient *b*	Coefficient *x0*
Gulf Toadfish (*Opsanus beta*)	68.19 ± 8.04[a]	0.33 ± 0.06[a]	1.23 ± 0.01[a]
Olive Flounder (*Paralichthys olivaceus*)	119.96 ± 14.6[b]	1.45 ± 0.2[b]	1.30 ± 0.01[b]
Yellowtail Snapper (*Ocyurus chrysurus*)	154.013 ± 25.4[b]	0.34 ± 0.08[a]	1.33 ± 0.01[b]

* Superscript letters denote significant differences between determined species values within respective columns ($p < 0.05$).

Table 3
Ichthyocarbonate dissolution rates (μeqv g^{-1} h^{-1}) at differing seawater aragonite saturation states (Ω_{arag}) among three marine teleost species. Values are determined from respective 2-parameter, exponential decay nonlinear regression fitted analyses for each species. 95 % confidence intervals are shown in squared brackets.

Species	$\Omega_{arag} = 1$	$\Omega_{arag} = 2$	$\Omega_{arag} = 3$	$\Omega_{arag} = 4$
Gulf Toadfish (*Opsanus beta*)	49.0 [19.6, 78.5]	35.2 [5.8, 64.7]	25.3 [−4.1, 54.8]	18.2 [−11.3, 47.7]
Olive Flounder (*Paralichthys olivaceus*)	28.1 [3.1, 53.2]	6.6 [−18.4, 31.6]	1.6 [−23.5, 26.6]	0.4 [−24.6, 25.4]
Yellowtail Snapper (*Ocyurus chrysurus*)	109.6 [45.7, 173.6]	78.0 [14.1, 142.0]	55.5 [−8.4, 119.5]	39.5 [−24.0, 103.5]

titration.

Overall, toadfish ichthyocarbonates had the lowest specific gravity of 1.23 ± 0.01 g·cm^{-3}, while both flounder and yellowtail snapper ichthyocarbonates were significantly less buoyant (1.30 ± 0.01 g·cm^{-3} and 1.33 ± 0.01 g·cm^{-3}, respectively) (Fig. 3, Table 2).

3.3. Fate of ichthyocarbonates in different ocean basins

Ichthyocarbonate diameter exerts a strong influence on dissolution depth as it affects sinking rate. To estimate the fraction of global fish ichthyocarbonate produced by each fish size class, we used the size distribution of global fish biomass (Jennings et al., 2008) and the scaling of ichthyocarbonate production rate with fish size (Wilson et al., 2009). Again, assuming that the three species examined here are representative of marine teleost fish in general, results revealed that 50 % of global ichthyocarbonate production is attributable to fish <0.001 g, 25 % is produced by fish 0.001–0.01 g, and the final remaining 25 % is attributed to fish >0.01 g (Fig. 4). Extrapolating the relationship between fish mass and ichthyocarbonate size derived here (Fig. 1), we estimated the median ichthyocarbonate diameters for these three size classes (0.25, 0.36, and 0.91 mm, respectively). Model estimates also predict residence times in oceanic settings between 2 and 35 days depending on diameter and the species from which it was excreted (Table 4) assuming ichthyocarbonate production and excretion near the ocean surface. Concerning fate (again assuming surface excretion), ichthyocarbonates similar to those produced by flounder that are 0.91 mm or larger in diameter are predicted to consistently reach depths below ranges

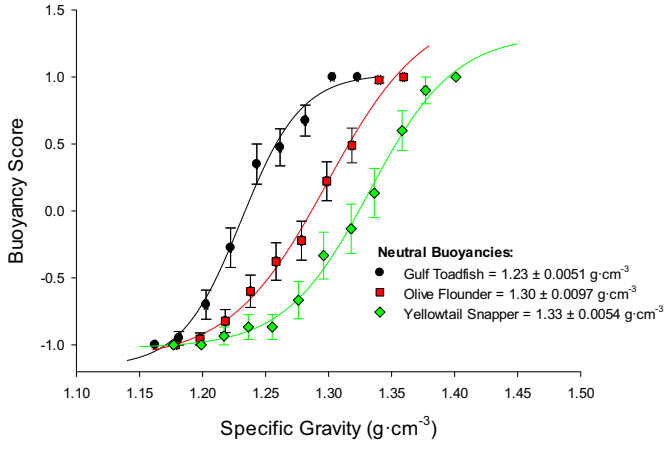

Fig. 3. Ichthyocarbonate specific gravity. Ichthyocarbonates from each tested species were placed in solutions of a range of specific gravities and given a buoyancy score (1-float, 0-suspended, −1-sink). Average buoyancy scores for species specific ichthyocarbonates were then plotted against solution specific gravity and a nonlinear regression 4-parameter sigmoidal equation was applied to determine specific gravity values equating to neutral buoyancy of the ichthyocarbonates. For regression analyses, r^2 values ranged from 0.995 to 0.998. Total number (n) of ichthyocarbonates of each species measured for specific gravity ranged from 30–45. Legend data is presented as each species ichthyocarbonate specific gravity at neutral buoyancy ± standard error.

associated with regional permanent thermoclines (~ 200–2000 m) (Carlson et al., 2010; Lampitt et al., 2008; Passow and Carlson, 2012) regardless of basin analyzed (Fig. 5). Ichthyocarbonates similar to those produced by yellowtail snapper and toadfish are generally predicted to fully dissolve at shallower depths - although larger ichthyocarbonates similar to those produced by both species (0.36–0.91+ mm) are predicted to reach depths of ~300–450 m prior to complete dissolution in certain ocean basins. Between basins, the Atlantic overall favors deeper fates before full dissolution, while the Pacific and Indian basins favor quicker ichthyocarbonate dissolution and shallower fates. Concerning the North Atlantic Ocean basin, percentages of combined ichthyocarbonate reaching depth again highlights ichthyocarbonates similar to those produced by flounder to be robust and reaching deeper depths before dissolution, with ~12.8 % reaching 1000+ m, while a similar proportion of ichthyocarbonate similar to those produced by both toadfish and yellowtail snapper reliably surpassed depths of only ~200 m (16.2 % and 13.1 %, respectively) before dissolving (Table 4).

4. Discussion

Based on the species examined here, ichthyocarbonates have higher dissolution rates compared to other biogenic carbonates (e.g., coral). Taking ichthyocarbonate diameter, specific gravity, and dissolution rates from these three species into account, we show that the majority of global ichthyocarbonates released near the surface dissolve in the upper water column (<500 m), and thereby likely contribute to active carbonate cycling in shallow oceans (Subhas et al., 2022) – a significant finding which reshapes current understandings of fish contributions to global inorganic carbon cycling. However, a significant fraction of global ichthyocarbonate production from some species is expected to reach depths past regional thermoclines (Table 4), while select species ichthyocarbonate may reach depths exceeding the aragonite saturation horizon in the Pacific and Indian Ocean basins (Fig. 5). Technological advances have led to a ~ 5× higher estimated global fish biomass (Bianchi et al., 2021), suggesting that annual carbonate production by marine fish likely exceeds previous estimates of production magnitudes (Wilson et al., 2009), making it even more important than previously appreciated to define the role of ichthyocarbonate in the global carbon cycle.

4.1. Ichthyocarbonate size and chemical composition

Previous studies have hypothesized that a relationship between fish mass and ichthyocarbonate size may exist (Salter et al., 2014), however, before this study, such a relationship has never been demonstrated. The three species examined presently adhere to a common relationship between fish mass and ichthyocarbonate diameter suggesting that this relationship may apply broadly among fishes. Diameters of ichthyocarbonate produced by seven Bahamian fish species have previously been reported (Salter et al., 2014) and generally correspond to average diameters of ichthyocarbonate reported here. Unfortunately, limited information on fish size and the pre-treatment of ichthyocarbonate with bleach performed in the earlier study by Salter and co-workers preclude direct comparison with our results. Based on the analyses conducted by us and others (Wilson et al., 2009), the majority of global

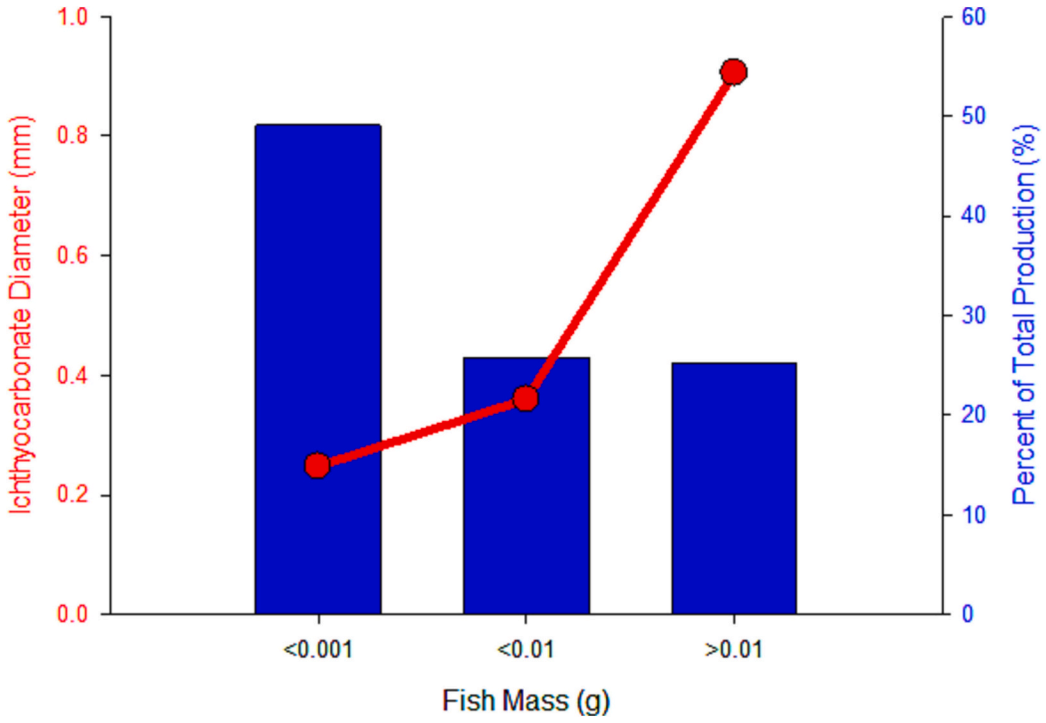

Fig. 4. Ichthyocarbonate size distributions and the relative contribution to estimated global ichthyocarbonate production across global fish size distribution. Ichthyocarbonate sizes were predicted from a generalized distribution of global fish biomass across fish size ranges (Jennings et al., 2008) and median fish size in grams for each of the size classes reported using fish mass-ichthyocarbonate diameter relationships determined in the present study.

ichthyocarbonate production is by fish smaller than those examined here and we accept uncertainty about the exact size of ichthyocarbonates produced by small individuals. However, it is a given that smaller fish will excrete ichthyocarbonates of smaller size, (assumed here), as ichthyocarbonate size is dictated by the size of the rectal opening. Thus, while we report a tight relationship between fish mass and ichthyocarbonate size (Fig. 1), further work is needed to determine if this relationship applies across all marine fish and sizes. It is possible that fish physiology, diet, and lifestyle could all play significant roles in dictating ichthyocarbonate size.

Previous analyses on seven Bahamian reef fish species determined that median ichthyocarbonate lengths at the point of excretion ranged between 0.03 and 3.63 mm (Salter et al., 2014). While no relationship with fish mass was reported, the authors noted that within species, bimodal distributions in carbonate grain lengths may suggest a correlative relationship with fish body size and carbonate size. However, deviations from this relationship occurred when comparing among species (i.e., occasional large ichthyocarbonate excretion in smaller species of fish; Salter et al., 2014). Our current analyses demonstrate that carbonate size is an important parameter to include in global ichthyocarbonate fate estimates.

Earlier analyses of ichthyocarbonate composition have revealed high concentrations of Mg^{2+} across ichthyocarbonate produced by various species, and thus they have been classified as high- to very high magnesium calcites (HMC or VHMC) (Perry et al., 2011; Salter et al., 2014, 2017; Walsh et al., 1991). Although the morphology of crystallites that comprise ichthyocarbonate may vary greatly between species (Perry et al., 2011; Salter et al., 2012, 2018, 2019), fish produced HMC (> 5 mol% $MgCO_3$) deviate from carbonate produced by coral, coccolithophores, and foraminifera which typically precipitate aragonite or low-magnesium calcite (LMC) when constructing their shells and skeletons - with LMC favored especially in cooler, temperate waters (Andersson et al., 2008; Morse et al., 1997; Stanley and Hardie, 1998). Mg^{2+} content in teleost ichthyocarbonates, however, can vary broadly both among and within fish families (Salter et al., 2018). For example, in the Gulf toadfish alone, our AAS results for tank-collected ichthyocarbonate indicate a mol%$MgCO_3$ content of 32.3 ± 0.8 (Table 1), while ichthyocarbonate collected directly from the intestine has been reported to have a mol%$MgCO_3$ content as high as 46–47 % (Heuer et al., 2012; Walsh et al., 1991). Large variability in mol%$MgCO_3$ is not uncommon. Assessments of tropical fish ichthyocarbonate collected off the coast of the Bahamas and the Great Barrier Reef in Australia further show mol% $MgCO_3$ can vary within ichthyocarbonate produced by a single fish family by >20 mol%$MgCO_3$ (Salter et al., 2018). Although median mol% $MgCO_3$ in ichthyocarbonate produced within fish families is predictable, with most occurring between approximately 30–40 % (Perry et al., 2011; Salter et al., 2018), overall mol%$MgCO_3$ can reach values as high as 100 % in ichthyocarbonate comprised predominantly of amorphous calcium magnesium carbonate (ACMC) (Salter et al., 2018). Our current analyses agree with this previously reported range, while reports for seawater acclimated Japanese eels (*Anguilla japonica*) (Mekuchi et al., 2010) also determined ichthyocarbonate mol% $MgCO_3$ in the ~20 % range. We speculate that differences among species ichthyocarbonate Mg^{2+} content may be a product of diet, physiology, and lifestyle (or any combination of these or more elements). In addition, we cannot exclude that variation among intestinal ichthyocarbonates and ichthyocarbonates collected at different times post excretion may contribute to changes in mol%$MgCO_3$ caused by dissolution. Thus, more work is needed to elucidate both abiotic and biotic factors which affect ichthyocarbonate composition.

4.2. Ichthyocarbonate dissolution and buoyancy

Compositional characteristics, including mineralogy, mol%$MgCO_3$ content, ichthyocarbonate buoyancy in marine waters, and/or organic matter coatings on ichthyocarbonate, may be important controls on rapid dissolution rates (Fig. 3), and thus the role of marine fish in the inorganic carbon cycle. Biogenic HMC (including ichthyocarbonate) is known to be more soluble than other carbonate minerals, such as aragonite and low-magnesium calcite, which have lower mol%$MgCO_3$

Table 4
North Atlantic Ocean water column residence times and depths before full dissolution for ichthyocarbonates (0.25, 0.36, and 0.91 mm in diameter) produced by three teleost species of marine fish.

Species	Cumulative Time in Water Column (Days)	Percentage of Combined Ichthyocarbonate Persisting to Depth			
		50 m	100 m	200 m	1000 m
Gulf Toadfish (*Opsanus beta*)					
0.25 mm	6.3				
0.36 mm	9.1	23.3%	21.3%	16.2%	0.0%
0.91 mm	15.6				
Olive Flounder (*Paralichthys olivaceus*)					
0.25 mm	35.3				
0.36 mm	35.5	96.3%	91.4%	72.2%	12.8%
0.91 mm	27.6				
Yellowtail Snapper (*Ocyurus chrysurus*)					
0.25 mm	2.9				
0.36 mm	4.2	22.7%	19.9%	13.1%	0.0%
0.91 mm	6.2				

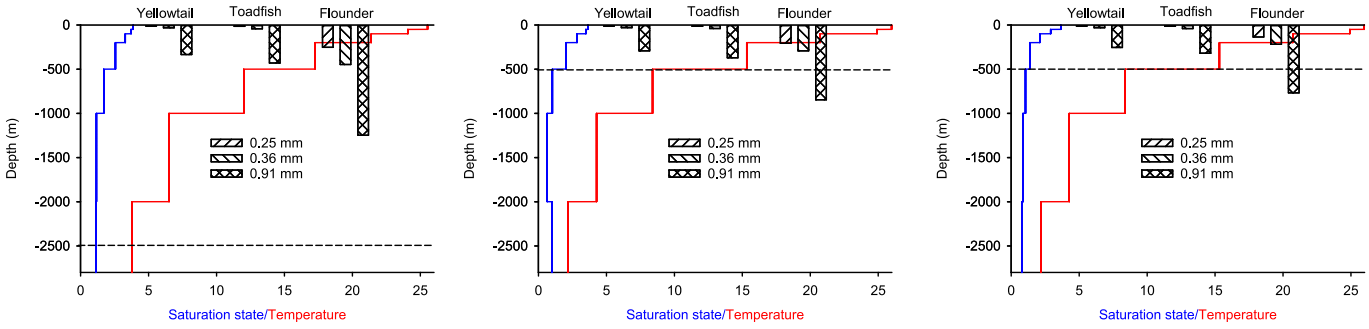

Fig. 5. Ichthyocarbonate dissolution depth modelling for three major ocean basins along with temperature (red) and aragonite saturation state (blue) profiles. Ichthyocarbonate sinking rates were calculated from specific gravity and size using buoyant velocity integrated approaches assuming seawater specific gravity of 1.030 g·ml^{-1} at 20 °C. From the sinking rates, depth at time post release was calculated and related to mean aragonite saturation and temperature depth profiles at 0, 50, 100, 200, 500, 1000, 2000, and 3000 m depths modeled in regions spanning 10° N to 30° N latitude in the Atlantic, Pacific, and Indian oceans (from Jiang et al., 2015). Dissolution rates were calculated as a function of time post excretion and the depths of full dissolution of ichthyocarbonates were determined. Dotted horizontal line represents the aragonite saturation horizon for each respective ocean basin.

content by contrast (Bischoff et al., 1987; Plummer and Mackenzie, 1974). Overall, prior experiments have shown that HMC under lab conditions is less stable (higher stoichiometric solubility product constants, pK^{*}_{sp}, and lower pK values) and more readily soluble in seawater compared to other carbonate polymorphs like aragonite and low-magnesium calcite (Morse et al., 2007). Toadfish ichthyocarbonates specifically have been shown to be 1.95× more soluble in seawater than aragonite (Woosley et al., 2012), while ACMC rich ichthyocarbonates produced by the gilt-head seabream (*Sparus aurata*) have been shown to dissolve ~2-fold faster than ground coral (whose skeletons are primarily composed of aragonite; Foran et al., 2013). Our results suggest that mol %$MgCO_3$ is not the first-order control on ichthyocarbonate dissolution rate (Table 1, Fig. 3). Ichthyocarbonate produced by yellowtail snapper contained the lowest Mg^{2+} concentrations (~22 mol% $MgCO_3$; Table 1) and consistently dissolved the fastest (Fig. 3), while ichthyocarbonate produced by the Olive flounder contained intermediate mol% $MgCO_3$ (~24.5 %, Table 1) and dissolved the slowest under the range of oceanic conditions tested. In fact, significant species-specific differences in

dissolution rate of ichthyocarbonate were observed, with enhanced dispersion at higher Ω_{arag} (Fig. 3). Thus, although oceanic surface waters are supersaturated ($\Omega_{arag} > 1$, often >3) with respect to aragonite and calcite, decreases in Ω_{arag} with depth as a result of changes in temperature, pH, and pressure (Dong et al., 2018; Feely et al., 2009; Jiang et al., 2015; Woosley et al., 2012) will likely exert an important influence on ichthyocarbonate fate when production by various species is considered. Although some conclude otherwise (see Subhas et al., 2022), previous studies have shown evidence that dissolution of carbonate minerals occurs above the aragonite saturation horizon (Feely et al., 2002; Milliman et al., 1999), leading those to speculate that a highly soluble $CaCO_3$ form may be responsible; biogenic HMC produced by fish now being recognized as a probable candidate (Salter et al., 2017; Wilson et al., 2009; Woosley et al., 2012). Our analyses determining high ichthyocarbonate dissolution rates over a range of seawater Ω_{arag}, including those >1, support this conclusion (Fig. 3).

In addition to ichthyocarbonate mineralogy and mol%$MgCO_3$ content, two other inherent factors implicated in ichthyocarbonate dissolution and fate are particle density/buoyancy and organic matter coatings. Ichthyocarbonate specific gravity governs the time it spends traversing the water column but has not been documented prior to the present study. Dominant forms of marine carbonate minerals (aragonite, low-magnesium calcite) have densities much higher than seawater, and thus readily sink when in their pure inorganic form (Gangstø et al., 2008; Subhas et al., 2022). Increasing carbonate Mg^{2+} content also slightly increases its density, resulting in higher density measurements for aragonite and pure $MgCO_3$ (~ 2.95 g·cm^{-3} and 2.96 g·cm^{-3}, respectively) compared to low magnesium calcite (2.71 g·cm^{-3}) (MacDonald, 1956). Interestingly, specific gravity of ichthyocarbonates for the three species examined here ranged between 1.23 and 1.33 g·cm^{-3}, despite their higher mol% $MgCO_3$ content (Table 1). This implies that some structural or physiochemical component present within or on ichthyocarbonates affects their buoyancy in the water column. One such component is the mucus sheath enveloping ichthyocarbonates at the point of excretion (Perry et al., 2011; Walsh et al., 1991), which likely reduces overall specific gravity. Another biological component that may affect specific gravity is microbiological communities (Walsh et al., 1991). Although Walsh et al. (1991) concluded that microbial communities do not enhance ichthyocarbonate production rates, additional work is needed to determine if these communities mediate calcification processes, as seen in microbialites (Chafetz and Buczynski, 1992; Dupraz et al., 2009; González-Muñoz et al., 2008; Rivadeneyra et al., 2006), or through metabolic processes affecting dissolution of carbonate precipitates (Godoi et al., 2009; Jansen et al., 2002; Milliman et al., 1999). Regardless, these organic components in ichthyocarbonate are theorized to differentially affect buoyancy properties and ichthyocarbonate structures (e.g., differential particle porosity), resulting in reduced carbonate specific gravity observed here. Proteinaceous organic matrices have also been shown to comprise ichthyocarbonates in marine teleost species and ultimately affect particle dissolution uniformity (Foran et al., 2013), wherein mineral nucleation rates have additionally been shown to be modulated by this matrix (Schauer et al., 2016, 2018; Schauer and Grosell, 2017). Effects of organic matrices and coatings on dissolution and ichthyocarbonate fate represent an important area of future investigation.

4.3. Ichthyocarbonate fate

With the assumption that the three species examined here are broadly representative of marine teleost fishes and that the influence of fish size on ichthyocarbonate diameter extends to fish smaller than those measured here, our fate modelling efforts for the three major ocean basins (Atlantic, Pacific, and Indian) collectively show that ichthyocarbonate contributes to both the shallow ocean carbonate cycle and the deep ocean alkalinity budget. Based on ichthyocarbonate produced by the three examined species and assuming both surface excretion and broad representation of marine fishes, most ichthyocarbonate is anticipated to dissolve within 200–500 m of its excretion depth (Table 4 and Fig. 5). Compared to ~50-day residence times of low-magnesium calcite in undersaturated waters at 5000 m water depth (Sarmiento, 2006), our model results predict that all ichthyocarbonate examined here will be characterized by residence times between 2 and 35 days (Table 4), despite the majority of the transit predicted to occur in supersaturated waters (Fig. 5). Ichthyocarbonate diameter/size appears to exert the greatest influence on ichthyocarbonate dissolution depth, though ocean Ω_{arag} also drives particle dissolution and ultimately fate (Fig. 5). Correspondingly, the depth of ichthyocarbonate dissolution is a product of the particles dissolution rate and specific gravity. However, it should be noted that while both factors contribute to ichthyocarbonate depth dissolution profiles, differences in ichthyocarbonate specific gravity among the three species tested was relatively modest (1.23–1.33 g cm^{-3}; Fig. 3) compared to dissolution rate (e.g., 28.14–109.62 μeqv g^{-1} h^{-1} at $\Omega_{arag} = 1$, Table 3) and that dissolution rates for additional species are sorely needed. Current estimates of collective preindustrial global fish biomass have increased to approximately 5.0–10.5 Gt (Bianchi et al., 2021); up from previous estimates of 0.8–2.05 Gt (Wilson et al., 2009). Of this, 3.5–7.4 Gt of marine fish biomass (~ 70 %; Jennings et al., 2008) is estimated to produce ichthyocarbonates between 0.125 and 2.0 mm in size. However, further breakdown incorporating presently determined fish mass-ichthyocarbonate diameter relationships reveal that 50 % of produced ichthyocarbonate (fish ≤0.001 g) is ≤0.25 mm in diameter, while a quarter of the excreted ichthyocarbonate is estimated to be 0.25–0.36 mm in diameter (fish 0.001–0.01 g) and the final quarter of the produced ichthyocarbonate is >0.91 mm in diameter (fish >0.01 g; Fig. 4). Considering this, and again assuming near surface excretion and that the species studied are broadly representative, our fate model presently predicts that most ichthyocarbonate fully dissolves prior to 500 m in all ocean basins analyzed. This ichthyocarbonate dissolution could account for upper and mesopelagic ocean alkalinity-depth profiles; enigmatic observations which have historically puzzled oceanographers (Sulpis et al., 2021; Wilson et al., 2009; Woosley et al., 2012). By factoring in mesopelagic fish – estimated to be the largest vertebrate biomass on the planet at 1.81–15.96 Gt (Irigoien et al., 2014; Proud et al., 2019) – carbonate production at depth and subsequent alkalinity pumps during vertical feeding migrations (Boyd et al., 2019; Cavan et al., 2019; Roberts et al., 2017), the importance of understanding the contribution of fish to oceanic alkalinity budgets becomes clear.

Considering ichthyocarbonate produced by the three species examined here and the presented relationship between fish size and ichthyocarbonate diameter are also representative of smaller individuals, we modeled the potential fate of ichthyocarbonate produced in the euphotic zone of the Atlantic Ocean. We estimate that a significant fraction of ichthyocarbonate produced in the surface ocean will reach the top of the mesopelagic zone and/or the minimum depths associated with regional thermoclines (200 m) (Table 4) (Lampitt et al., 2008). A smaller but not insignificant amount (13 % of ichthyocarbonates with characteristics similar to those of the flounder studied here) is predicted to reach depths of 1000 m, a depth widely cited to reflect millennial-scale sequestration in the deep ocean (Bianchi et al., 2021; Boyd et al., 2019). Variability in size, specific gravity, and dissolution rates of ichthyocarbonate observed here suggests that the composition of the sinking material will vary based on the ultimate proportions contributed by specific species, as well as the depth at which the composition of the flux is considered. Importantly, ichthyocarbonate will be excreted at varying depths by marine fish of different lifestyles, including, for example, diel vertically migrating mesopelagic species (Boyd et al., 2019; Cavan et al., 2019; Roberts et al., 2017), which will likely result in deeper dissolution depths of ichthyocarbonate produced by some species than presented here. However, our calculations provide conservative and important preliminary insight into the relative contributions of ichthyocarbonate to shallow carbonate cycling and vertical alkalinity profiles. Results particularly highlight the importance of quantifying

interspecies variability in ichthyocarbonate composition and dissolution rate to enhance predictions of ichthyocarbonate fate in natural environments, and thus the role of ichthyocarbonate in the global carbon cycle.

4.4. Limitations and future considerations

The analyses presented here are the first to model ichthyocarbonate dissolution depth and fate, however, results are limited to three species of a relatively narrow size range. Currently, our analyses incorporate ichthyocarbonate produced by species inhabiting benthic or relatively shallow habitats. Although all marine teleost species examined to date produce ichthyocarbonate, composition, production, and morphology can drastically differ among fishes (Ghilardi et al., 2023; Salter et al., 2018). Thus, when extending this variability to fishes inhabiting differing pelagic zones (*epi* -versus meso- versus bathy- or abyssopelagic) or across species lifestyles and climate zones, it becomes readily apparent that further research on ichthyocarbonate composition, production, and physiochemistry across a greater breadth of fish species and sizes is needed to accurately determine the impact of marine fish contributions to the global carbon cycle. Such endeavors, despite their numerous challenges, are needed to ensure that more complete models are constructed to define ichthyocarbonate fate in oceanic environments. Similarly, variations in diet are suspected to significantly affect ichthyocarbonate physiochemical properties and production rates. Marine fish intestinal lumen Ca^{2+} and Mg^{2+} concentrations are tied to diet and ambient seawater concentrations, where changes in concentration of these two divalent cations directly impacts ichthyocarbonate precipitation (Mekuchi et al., 2010; Wilson and Grosell, 2003). Despite findings of satiation state and functional group (and assumed diet) having no effect on ichthyocarbonate composition and precipitation polymorph type in reef species (Salter et al., 2012, 2017), other components controlling ichthyocarbonate production and physiochemical properties may be affected by diet. These components include i.) rates of cation absorption across fish intestinal epithelium; ii.) microbiota incorporation and impacts on carbonate structure and porosity; iii) differential effects on fish metabolic rate and thereby ichthyocarbonate production; iv) impacts on mucus production and proteinaceous matrixes associated with ichthyocarbonates.

Two unaccounted for physical properties of seawater in our current analyses are thought to potentially impact ichthyocarbonate status within the water column and therefore fate: water temperature and pH. While our current modelling parameters included temperature impacts on water viscosity, it is unknown how water temperatures may impact ichthyocarbonate dissolution and buoyancy. Although heightened water temperatures have been found to increase ichthyocarbonate production in numerous marine species (due to impacts on fish metabolic rate; Ghilardi et al., 2023; Heuer et al., 2016; Wilson et al., 2009), temperature and pH impacts on dissolution rate and buoyancy of fish-derived carbonate sources remain unstudied. Conceivably, warmer seawater temperatures and decreased pH might enhance ichthyocarbonate dissolution rates (and vice versa), as is similarly observed for other carbonate polymorphs (Adkins et al., 2021; Alkattan et al., 1998; Gautelier et al., 1999; Naviaux et al., 2019; Sjöberg and Rickard, 1984). Interestingly, reef fish species inhabiting cooler, temperate waters at higher latitudes have been shown to produce greater quantities of less soluble forms of calcite (LMC) compared to the same or similar species in warmer waters which tended to favor production of more soluble compositions, including HMC and ACMC (Salter et al., 2019). Correlations between ichthyocarbonate mineralogy (and its solubility) and environmental temperature remains poorly understood. Further, effects of changing temperature and pH through the water column on ichthyocarbonate buoyancy - and other intrinsic properties including microbial content/structure –additionally requires further investigation.

Lastly, two future parameters whose incorporation would potentially refine our modelling efforts are ichthyocarbonate shape and water column pressure. Currently, our model assumes spherical shapes when ichthyocarbonate from different fish species may take on more cylindrical or irregular morphologies. Considering shape has experimentally been shown to impact and change theoretical sinking rate estimates for numerous biotic and abiotic solids in aquatic systems, including phytoplankton and microplastics (Durante et al., 2019; Kowalski et al., 2016; Liu et al., 2022; Padisák et al., 2003), incorporating ichthyocarbonate shape into modelling efforts may better elucidate sinking properties associated with ichthyocarbonate. Water pressure has been shown to kinetically enhance calcite dissolution for pressures 10–700 dbar (above 700 and up to 2500 dbar, dissolution rates become independent of pressure; Dong et al., 2018). Increases in hydrostatic pressure have additionally been shown to decrease microbial function with increasing pressure, ultimately reducing substrate dissolution (Tamburini et al., 2006, 2009). Given the marked presence of bacteria in ichthyocarbonate (Walsh et al., 1991) and their assumed contribution to precipitate decomposition and dissolution, pressure impacts on microbe enzymatic processes and function may substantially influence dissolution properties. Such elements – ichthyocarbonate shape and water pressure included – and their interplay with each other undoubtedly affect fate and influence of ichthyocarbonate on oceanic carbon cycles.

5. Conclusions

For the first time, we determined relationships between fish mass and ichthyocarbonate size, measure ichthyocarbonate specific gravity, and dissolution rates. These observations allowed us to provide the first estimates of ichthyocarbonate sinking rates and predict the depths of their complete dissolution based on characteristics of ichthyocarbonates produced by three fish species within a relatively narrow size range. Ichthyocarbonate specific gravity ranged from 1.23 to 1.33 g/cm^3, while dissolutions rates varied by species and were dependent on aragonite saturation state. When environmental parameters of the Atlantic, Pacific, and Indian Oceans are considered, our observations based on three teleost species suggest that ichthyocarbonates $\leq$0.36 mm in diameter (size of precipitates accounting for 75 % of global production) are likely to fully dissolve before reaching 500 m in depth. However, ichthyocarbonates $\geq$0.91 mm in diameter (25 % of all precipitates formed globally) from some species reach depths beyond 1000 m. Considering estimated global carbonate production magnitudes, results indicate that marine fish contribute significantly to shallow ocean carbonate cycling and to the definition of vertical alkalinity profiles in contemporary oceans. Notably, elevated CO_2 enhances intestinal HCO_3^- secretion and ichthyocarbonate production (Gregório et al., 2019; Heuer et al., 2012, 2016; Heuer and Grosell, 2016), thus, marine fish and ichthyocarbonate are expected to be integral to the oceanic response to rising concentrations of atmospheric CO_2.

CRediT authorship contribution statement

Erik J. Folkerts: Conceptualization, Data curation, Formal analysis, Investigation, Methodology, Validation, Visualization, Writing – original draft, Writing – review & editing. **Amanda M. Oehlert:** Conceptualization, Data curation, Formal analysis, Funding acquisition, Project administration, Supervision, Writing – original draft, Writing – review & editing. **Rachael M. Heuer:** Conceptualization, Investigation, Project administration, Visualization, Writing – review & editing. **Sandy Nixon:** Data curation, Formal analysis, Investigation, Writing – review & editing. **John D. Stieglitz:** Conceptualization, Project administration, Supervision, Writing – review & editing. **Martin Grosell:** Conceptualization, Data curation, Formal analysis, Funding acquisition, Investigation, Project administration, Supervision, Visualization, Writing – original draft, Writing – review & editing.

Declaration of competing interest

The authors declare that they have no known competing financial interests or personal relationships that could have appeared to influence the work reported in this paper.

Data availability

Data will be made available on request.

Acknowledgements

E.J.F. is supported through a Natural Sciences and Engineering Research Council of Canada Postdoctoral Fellowship (PDF-557505-2021). A.M.O acknowledges start-up funds provided by the Rosenstiel School of Marine, Atmospheric, and Earth Sciences at the University of Miami. M.G. is a Maytag Chair of Ichthyology. A.M.O. and M.G. are supported by the National Science Foundation (NSF-OCE-2319245).

References

Adkins, J.F., Naviaux, J.D., Subhas, A.V., Dong, S., Berelson, W.M., 2021. The dissolution rate of $CaCO_3$ in the ocean. Annu. Rev. Mar. Sci. 13, 57–80. https://doi.org/10.1146/annurev-marine-041720-092514.

Alkattan, M., Oelkers, E.H., Dandurand, J.-L., Schott, J., 1998. An experimental study of calcite and limestone dissolution rates as a function of pH from −1 to 3 and temperature from 25 to 80 °C. Chem. Geol. 151, 199–214. https://doi.org/10.1016/S0009-2541(98)00080-1.

Andersson, A., Mackenzie, F., Bates, N., 2008. Life on the margin: implications of ocean acidification on Mg-calcite, high latitude and cold-water marine calcifiers. Mar. Ecol. Prog. Ser. 373, 265–273. https://doi.org/10.3354/meps07639.

Berner, R.A., 2001. GEOCARB III: a revised model of atmospheric CO_2 over Phanerozoic time. Am. J. Sci. 301, 182–204. https://doi.org/10.2475/ajs.301.2.182.

Bianchi, D., Carozza, D.A., Galbraith, E.D., Guiet, J., DeVries, T., 2021. Estimating global biomass and biogeochemical cycling of marine fish with and without fishing. Sci. Adv. 7, eabd7554 https://doi.org/10.1126/sciadv.abd7554.

Bischoff, W.D., Mackenzie, F.T., Bishop, F.C., 1987. Stabilities of synthetic magnesian calcites in aqueous solution: comparison with biogenic materials. Geochim. Cosmochim. Acta 51, 1413–1423. https://doi.org/10.1016/0016-7037(87)90325-5.

Boyd, P.W., Claustre, H., Levy, M., Siegel, D.A., Weber, T., 2019. Multi-faceted particle pumps drive carbon sequestration in the ocean. Nature 568, 327–335. https://doi.org/10.1038/s41586-019-1098-2.

Brix, K.V., Wood, C.M., Grosell, M., 2013. Measuring titratable alkalinity by single versus double endpoint titration: an evaluation in two cyprinodont species and implications for characterizing net H^+ flux in aquatic organisms. Comp. Biochem. Physiol. A Mol. Integr. Physiol. 164, 221–228. https://doi.org/10.1016/j.cbpa.2012.09.010.

Broecker, W.S., 2009. Wally's quest to understand the ocean's $CaCO_3$ cycle. Annu. Rev. Mar. Sci. 1, 1–18. https://doi.org/10.1146/annurev.marine.010908.163936.

Buesseler, K.O., Boyd, P.W., Black, E.E., Siegel, D.A., 2020. Metrics that matter for assessing the ocean biological carbon pump. Proc. Natl. Acad. Sci. 117 (18), 9679–9687. https://doi.org/10.1073/pnas.1918114117.

Buitenhuis, E.T., Le Quéré, C., Bednaršek, N., Schiebel, R., 2019. Large contribution of Pteropods to shallow $CaCO_3$ export. Glob. Biogeochem. Cycles 33, 458–468. https://doi.org/10.1029/2018GB006110.

Carlson, C.A., Hansell, D.A., Nelson, N.B., Siegel, D.A., Smethie, W.M., Khatiwala, S., Meyers, M.M., Halewood, E., 2010. Dissolved organic carbon export and subsequent remineralization in the mesopelagic and bathypelagic realms of the North Atlantic basin. Deep-Sea Res. II Top. Stud. Oceanogr. 57, 1433–1445. https://doi.org/10.1016/j.dsr2.2010.02.013.

Carter, B.R., Feely, R.A., Lauvset, S.K., Olsen, A., DeVries, T., Sonnerup, R., 2021. Preformed properties for marine organic matter and carbonate mineral cycling quantification. Glob. Biogeochem. Cycles 35. https://doi.org/10.1029/2020GB006623.

Cavan, E.L., Laurenceau-Cornec, E.C., Bressac, M., Boyd, P.W., 2019. Exploring the ecology of the mesopelagic biological pump. Prog. Oceanogr. 176, 102125 https://doi.org/10.1016/j.pocean.2019.102125.

Chafetz, H.S., Buczynski, C., 1992. Bacterially induced lithification of microbial mats. PALAIOS 7, 277. https://doi.org/10.2307/3514973.

Doney, S.C., Fabry, V.J., Feely, R.A., Kleypas, J.A., 2009. Ocean acidification: the other CO_2 problem. Annu. Rev. Mar. Sci. 1, 169–192. https://doi.org/10.1146/annurev.marine.010908.163834.

Dong, S., Subhas, A.V., Rollins, N.E., Naviaux, J.D., Adkins, J.F., Berelson, W.M., 2018. A kinetic pressure effect on calcite dissolution in seawater. Geochim. Cosmochim. Acta 238, 411–423. https://doi.org/10.1016/j.gca.2018.07.015.

Ducklow, H., Steinberg, D., Buesseler, K., 2001. Upper Ocean carbon export and the biological pump. Oceanog 14, 50–58. https://doi.org/10.5670/oceanog.2001.06.

Dupraz, C., Reid, R.P., Braissant, O., Decho, A.W., Norman, R.S., Visscher, P.T., 2009. Processes of carbonate precipitation in modern microbial mats. Earth Sci. Rev. 96, 141–162. https://doi.org/10.1016/j.earscirev.2008.10.005.

Durante, G., Basset, A., Stanca, E., Roselli, L., 2019. Allometric scaling and morphological variation in sinking rate of phytoplankton. J. Phycol. 55, 1386–1393. https://doi.org/10.1111/jpy.12916.

Evans, D.H., Piermarini, P.M., Choe, K.P., 2005. The multifunctional fish gill: dominant site of gas exchange, osmoregulation, acid-base regulation, and excretion of nitrogenous waste. Physiol. Rev. 85, 97–177. https://doi.org/10.1152/physrev.00050.2003.

Feely, R.A., Sabine, C.L., Lee, K., Millero, F.J., Lamb, M.F., Greeley, D., Bullister, J.L., Key, R.M., Peng, T.-H., Kozyr, A., Ono, T., Wong, C.S., 2002. In situ calcium carbonate dissolution in the Pacific Ocean. Glob. Biogeochem. Cycles 16. https://doi.org/10.1029/2002GB001866, 91-1-91–12.

Feely, R.A., Sabine, C.L., Lee, K., Berelson, W., Kleypas, J., Fabry, V.J., Millero, F.J., 2004. Impact of anthropogenic CO_2 on the $CaCO_3$ system in the oceans. Science 305, 362–366. https://doi.org/10.1126/science.1097329.

Feely, R.A., Doney, S.C., Cooley, S.R., 2009. Ocean acidification: present conditions and future changes in a high-CO_2 world. Oceanography 22, 36–47.

Foran, E., Weiner, S., Fine, M., 2013. Biogenic fish-gut calcium carbonate is a stable amorphous phase in the gilt-head seabream, *Sparus aurata*. Sci. Rep. 3, 1700. https://doi.org/10.1038/srep01700.

Frankignoulle, M., Canon, C., Gattuso, J.-P., 1994. Marine calcification as a source of carbon dioxide: positive feedback of increasing atmospheric CO_2. Limnol. Oceanogr. 39, 458–462. https://doi.org/10.4319/lo.1994.39.2.0458.

Frankignoulle, M., Pichon, M., Gattuso, J.P., 1995. Aquatic calcification as a source of carbon dioxide. In: Beran (Ed.), Carbon Sequestration in the Biosphere, NATO ASI Series. Springer, Berlin/Heidelberg.

Gangstø, R., Gehlen, M., Schneider, B., Bopp, L., Aumont, O., Joos, F., 2008. Modelling the Marine Aragonite Cycle: Changes under Rising Carbon Dioxide and its Role in Shallow Water $CaCO_3$ Dissolution.

Gattuso, J.P., Pichon, M., Delesalle, B., Frankignoulle, M., 1993. Community metabolism and air-sea CO_2 fluxes in a coral reef ecosystem (Moorea, French Polynesia). Mar. Ecol. Prog. Ser. 96, 259–267.

Gautelier, M., Oelkers, E.H., Schott, J., 1999. An experimental study of dolomite dissolution rates as a function of pH from −0.5 to 5 and temperature from 25 to 80 °C. Chem. Geol. 157, 13–26. https://doi.org/10.1016/S0009-2541(98)00193-4.

Ghilardi, M., Salter, M.A., Parravicini, V., Ferse, S.C.A., Rixen, T., Wild, C., Birkicht, M., Perry, C.T., Berry, A., Wilson, R.W., Mouillot, D., Bejarano, S., 2023. Temperature, species identity and morphological traits predict carbonate excretion and mineralogy in tropical reef fishes. Nat. Commun. 14, 985. https://doi.org/10.1038/s41467-023-36617-7.

Godoi, R.H.M., Aerts, K., Harlay, J., Kaegi, R., Ro, C.-U., Chou, L., Van Grieken, R., 2009. Organic surface coating on Coccolithophores - Emiliania huxleyi: its determination and implication in the marine carbon cycle. Microchem. J. 91, 266–271. https://doi.org/10.1016/j.microc.2008.12.009.

González-Muñoz, M.T., De Linares, C., Martínez-Ruiz, F., Morcillo, F., Martín-Ramos, D., Arias, J.M., 2008. Ca–Mg kutnahorite and struvite production by Idiomarina strains at modern seawater salinities. Chemosphere 72, 465–472. https://doi.org/10.1016/j.chemosphere.2008.02.010.

Gregório, S.F., Ruiz-Jarabo, I., Carvalho, E.M., Fuentes, J., 2019. Increased intestinal carbonate precipitate abundance in the sea bream (Sparus aurata L.) in response to ocean acidification. PLoS One 14, e0218473. https://doi.org/10.1371/journal.pone.0218473.

Grosell, M., 2006. Intestinal anion exchange in marine fish osmoregulation. J. Exp. Biol. 209, 2813–2827. https://doi.org/10.1242/jeb.02345.

Grosell, M., 2011. Intestinal anion exchange in marine teleosts is involved in osmoregulation and contributes to the oceanic inorganic carbon cycle: intestinal anion exchange in marine fish. Acta Physiol. 202, 421–434. https://doi.org/10.1111/j.1748-1716.2010.02241.x.

Grosell, M., Oehlert, A.M., 2023. Staying hydrated in seawater. Physiology 38, 178–188. https://doi.org/10.1152/physiol.00005.2023.

Grosell, M., Taylor, J.R., 2007. Intestinal anion exchange in teleost water balance. Comp. Biochem. Physiol. A Mol. Integr. Physiol. 148, 14–22. https://doi.org/10.1016/j.cbpa.2006.10.017.

Grosell, M., Mager, E.M., Williams, C., Taylor, J.R., 2009. High rates of HCO_3^- secretion and Cl^- absorption against adverse gradients in the marine teleost intestine: the involvement of an electrogenic anion exchanger and H^+-pump metabolon? J. Exp. Biol. 212, 1684–1696. https://doi.org/10.1242/jeb.027730.

Heuer, R.M., Grosell, M., 2016. Elevated CO_2 increases energetic cost and ion movement in the marine fish intestine. Sci. Rep. 6, 34480 https://doi.org/10.1038/srep34480.

Heuer, R.M., Esbaugh, A.J., Grosell, M., 2012. Ocean acidification leads to counterproductive intestinal base loss in the Gulf toadfish (*Opsanus beta*). Physiol. Biochem. Zool. 85, 450–459. https://doi.org/10.1086/667617.

Heuer, R.M., Munley, K.M., Narsinghani, N., Wingar, J.A., Mackey, T., Grosell, M., 2016. Changes to intestinal transport physiology and carbonate production at various CO_2 levels in a marine teleost, the Gulf toadfish (*Opsanus beta*). Physiol. Biochem. Zool. 89, 402–416. https://doi.org/10.1086/688235.

Honjo, S., Eglinton, T., Taylor, C., Ulmer, K., Sievert, S., Bracher, A., German, C., Edgcomb, V., Francois, R., Iglesias-Rodriguez, M.D., Van Mooy, B., Rapeta, D., 2014. Understanding the role of the biological pump in the global carbon cycle: an imperative for ocean science. Oceanography 27 (3), 10–16. https://doi.org/10.5670/oceanog.2014.78.

Iglesias-Rodriguez, M.D., Armstrong, R., Feely, R., Hood, R., Kleypas, J.A., Milliman, J.D., Sabine, C.L., Sarmiento, J., 2002. Progress made in study of ocean's calcium carbonate budget. EOS Trans. Am. Geophys. Union 83, 365–375.

Irigoien, X., Klevjer, T.A., Røstad, A., Martinez, U., Boyra, G., Acuña, J.L., Bode, A., Echevarria, F., Gonzalez-Gordillo, J.I., Hernandez-Leon, S., Agusti, S., Aksnes, D.L., Duarte, C.M., Kaartvedt, S., 2014. Large mesopelagic fishes biomass and trophic

efficiency in the open ocean. Nat. Commun. 5, 3271. https://doi.org/10.1038/ncomms4271.
Jansen, H., Zeebe, R.E., Wolf-Gladrow, D.A., 2002. Modelling the dissolution of settling $CaCO_3$ in the ocean. Glob. Biogeochem. Cycles 16. https://doi.org/10.1029/2000GB001279, 11-1-11–16.
Jennings, S., Mélin, F., Blanchard, J.L., Forster, R.M., Dulvy, N.K., Wilson, R.W., 2008. Global-scale predictions of community and ecosystem properties from simple ecological theory. Proc. R. Soc. B 275, 1375–1383. https://doi.org/10.1098/rspb.2008.0192.
Jiang, L.-Q., Feely, R.A., Carter, B.R., Greeley, D.J., Gledhill, D.K., Arzayus, K.M., 2015. Climatological distribution of aragonite saturation state in the global oceans. Glob. Biogeochem. Cycles 29, 1656–1673. https://doi.org/10.1002/2015GB005198.
Kowalski, N., Reichardt, A.M., Waniek, J.J., 2016. Sinking rates of microplastics and potential implications of their alteration by physical, biological, and chemical factors. Mar. Pollut. Bull. 109, 310–319. https://doi.org/10.1016/j.marpolbul.2016.05.064.
Lampitt, R.S., Achterberg, E.P., Anderson, T.R., Hughes, J.A., Iglesias-Rodriguez, M.D., Kelly-Gerreyn, B.A., Lucas, M., Popova, E.E., Sanders, R., Shepherd, J.G., Smythe-Wright, D., Yool, A., 2008. Ocean fertilization: a potential means of geoengineering? Phil. Trans. R. Soc. A 366, 3919–3945. https://doi.org/10.1098/rsta.2008.0139.
Langer, M.R., 2008. Assessing the contribution of Foraminiferan Protists to Global Ocean carbonate production. J. Eukaryot. Microbiol. 55, 163–169. https://doi.org/10.1111/j.1550-7408.2008.00321.x.
Lee, K., Millero, F.J., Byrne, R.H., Feely, R.A., Wanninkhof, R., 2000. The recommended dissociation constants for carbonic acid in seawater. Geophys. Res. Lett. 27, 229–232. https://doi.org/10.1029/1999GL002345.
Lewis, E., Wallace, D.W.R., Pierrot, D.E., 2006. MS excel program developed for CO_2 system calculations. ORNL/CDIAC-105a.
Liu, S., Huang, Y., Luo, D., Wang, X., Wang, Z., Ji, X., Chen, Z., Dahlgren, R.A., Zhang, M., Shang, X., 2022. Integrated effects of polymer type, size and shape on the sinking dynamics of biofouled microplastics. Water Res. 220, 118656 https://doi.org/10.1016/j.watres.2022.118656.
MacDonald, G.J.F., 1956. Experimental determination of calcite-aragonite equilibrium relations at elevated temperatures and pressures. Am. Mineral. 41, 744–756.
Marshall, W.S., Grosell, M., 2005. Ion transport, osmoregulation and acid–base balance. In: Evans, D.H., Claiborne, J.B. (Eds.), Physiology of Fishes. CRC Press, pp. 179–214.
Martin, A.H., Pearson, H.C., Saba, G.K., Olsen, E.M., 2021. Integral functions of marine vertebrates in the ocean carbon cycle and climate change mitigation. One Earth 4, 680–693. https://doi.org/10.1016/j.oneear.2021.04.019.
McDonald, M.D., Grosell, M., 2006. Maintaining osmotic balance with an aglomerular kidney. Comp. Biochem. Physiol. A Mol. Integr. Physiol. 143, 447–458. https://doi.org/10.1016/j.cbpa.2005.12.029.
Mehrbach, C., Culberson, C.H., Hawley, J.E., Pytkowicx, R.M., 1973. Measurement of the apparent dissociation constants of carbonic acid in seawater at atmospheric pressure 1. Limnol. Oceanogr. 18, 897–907. https://doi.org/10.4319/lo.1973.18.6.0897.
Mekuchi, M., Hatta, T., Kaneko, T., 2010. Mg-calcite, a carbonate mineral, constitutes ca precipitates produced as a byproduct of osmoregulation in the intestine of seawater-acclimated Japanese eel Anguilla japonica. Fish. Sci. 76, 199–205. https://doi.org/10.1007/s12562-009-0199-5.
Millero, F.J., 2005. Chemical Oceanography, 3rd ed. CRC Press, Boca Raton.
Millero, F.J., 2007. The marine inorganic carbon cycle. Chem. Rev. 107, 308–341. https://doi.org/10.1021/cr0503557.
Milliman, J.D., 1993. Production and accumulation of calcium carbonate in the ocean: budget of a nonsteady state. Glob. Biogeochem. Cycles 7, 927–957. https://doi.org/10.1029/93GB02524.
Milliman, J.D., Droxler, A.W., 1996. Neritic and pelagic carbonate sedimentation in the marine environment: ignorance is not bliss. Geol. Rundsch. 85, 496–504. https://doi.org/10.1007/BF02369004.
Milliman, J.D., Troy, P.J., Balch, W.M., Adams, A.K., Li, Y.-H., Mackenzie, F.T., 1999. Biologically mediated dissolution of calcium carbonate above the chemical lysocline? Deep-Sea Res. I Oceanogr. Res. Pap. 46, 1653–1669. https://doi.org/10.1016/S0967-0637(99)00034-5.
Morse, J.W., Wang, Q., Tsio, M.Y., 1997. Influences of temperature and Mg:Ca ratio on $CaCO_3$ precipitates from seawater. Geol 25, 85. https://doi.org/10.1130/0091-7613(1997)025<0085:IOTAMC>2.3.CO;2.
Morse, J.W., Arvidson, R.S., Lüttge, A., 2007. Calcium carbonate formation and dissolution. Chem. Rev. 107, 342–381. https://doi.org/10.1021/cr050358j.
Naviaux, J.D., Subhas, A.V., Rollins, N.E., Dong, S., Berelson, W.M., Adkins, J.F., 2019. Temperature dependence of calcite dissolution kinetics in seawater. Geochim. Cosmochim. Acta 246, 363–384. https://doi.org/10.1016/j.gca.2018.11.037.
Nowicki, M., DeVries, T., Siegel, D.A., 2022. Quantifying the carbon export and sequestration pathways of the ocean's biological carbon pump. Global Biogeochem. Cycles 36 (3). https://doi.org/10.1029/2021GB007083.
Orr, J.C., Fabry, V.J., Aumont, O., Bopp, L., Doney, S.C., Feely, R.A., Gnanadesikan, A., Gruber, N., Ishida, A., Joos, F., Key, R.M., Lindsay, K., Maier-Reimer, E., Matear, R., Monfray, P., Mouchet, A., Najjar, R.G., Plattner, G.-K., Rodgers, K.B., Sabine, C.L., Sarmiento, J.L., Schlitzer, R., Slater, R.D., Totterdell, I.J., Weirig, M.-F., Yamanaka, Y., Yool, A., 2005. Anthropogenic Ocean acidification over the twenty-first century and its impact on calcifying organisms. Nature 437, 681–686. https://doi.org/10.1038/nature04095.
Padisák, J., Soróczki-Pintér, É., Rezner, Z., 2003. Sinking properties of some phytoplankton shapes and the relation of form resistance to morphological diversity of plankton — An experimental study. In: Martens, K. (Ed.), Aquatic Biodiversity, Developments in Hydrobiology. Springer, pp. 243–257.
Pasparakis, C., Wang, Y., Heuer, R.M., Zhang, W., Stieglitz, J.D., McGuigan, C.J., Benetti, D.D., Scholey, V.P., Margulies, D., Grosell, M., 2022. Ultraviolet avoidance by embryonic buoyancy control in three species of marine fish. Sci. Total Environ. 806, 150542 https://doi.org/10.1016/j.scitotenv.2021.150542.
Passow, U., Carlson, C., 2012. The biological pump in a high CO_2 world. Mar. Ecol. Prog. Ser. 470, 249–271. https://doi.org/10.3354/meps09985.
Perry, C.T., Salter, M.A., Harborne, A.R., Crowley, S.F., Jelks, H.L., Wilson, R.W., 2011. Fish as major carbonate mud producers and missing components of the tropical carbonate factory. Proc. Natl. Acad. Sci. U. S. A. 108, 3865–3869. https://doi.org/10.1073/pnas.1015895108.
Plummer, L.N., Mackenzie, F.T., 1974. Predicting mineral solubility from rate data; application to the dissolution of magnesian calcites. Am. J. Sci. 274, 61–83. https://doi.org/10.2475/ajs.274.1.61.
Proud, R., Handegard, N.O., Kloser, R.J., Cox, M.J., Brierley, A.S., 2019. From siphonophores to deep scattering layers: uncertainty ranges for the estimation of global mesopelagic fish biomass. ICES J. Mar. Sci. 76, 718–733. https://doi.org/10.1093/icesjms/fsy037.
Ridgwell, A., Zeebe, R., 2005. The role of the global carbonate cycle in the regulation and evolution of the earth system. Earth Planet. Sci. Lett. 234, 299–315. https://doi.org/10.1016/j.epsl.2005.03.006.
Rivadeneyra, M.A., Martín-Algarra, A., Sánchez-Navas, A., Martíin-Ramos, D., 2006. Carbonate and phosphate precipitation by *Chromohalobacter marismortui*. Geomicrobiol J. 23, 89–101. https://doi.org/10.1080/01490450500533882.
Roberts, C.M., O'Leary, B.C., McCauley, D.J., Cury, P.M., Duarte, C.M., Lubchenco, J., Pauly, D., Sáenz-Arroyo, A., Sumaila, U.R., Wilson, R.W., Worm, B., Castilla, J.C., 2017. Marine reserves can mitigate and promote adaptation to climate change. Proc. Natl. Acad. Sci. U. S. A. 114, 6167–6175. https://doi.org/10.1073/pnas.1701262114.
Saba, G.K., Burd, A.B., Dunne, J.P., Hernández-León, S., Martin, A.H., Rose, K.A., Salisbury, J., Steinberg, D.K., Trueman, C.N., Wilson, R.W., Wilson, S.E., 2021. Toward a better understanding of fish-based contribution to ocean carbon flux. Limnol. Oceanogr. 66, 1639–1664. https://doi.org/10.1002/lno.11709.
Salter, M.A., Perry, C.T., Wilson, R.W., 2012. Production of mud-grade carbonates by marine fish: crystalline products and their sedimentary significance. Sedimentology 59, 2172–2198. https://doi.org/10.1111/j.1365-3091.2012.01339.x.
Salter, M.A., Perry, C.T., Wilson, R.W., 2014. Size fraction analysis of fish-derived carbonates in shallow sub-tropical marine environments and a potentially unrecognised origin for peloidal carbonates. Sediment. Geol. 314, 17–30. https://doi.org/10.1016/j.sedgeo.2014.10.005.
Salter, M.A., Harborne, A.R., Perry, C.T., Wilson, R.W., 2017. Phase heterogeneity in carbonate production by marine fish influences their roles in sediment generation and the inorganic carbon cycle. Sci. Rep. 7, 765. https://doi.org/10.1038/s41598-017-00787-4.
Salter, M.A., Perry, C.T., Stuart-Smith, R.D., Edgar, G.J., Wilson, R.W., Harborne, A.R., 2018. Reef fish carbonate production assessments highlight regional variation in sedimentary significance. Geology 46, 699–702. https://doi.org/10.1130/G45286.1.
Salter, M.A., Perry, C.T., Smith, A.M., 2019. Calcium carbonate production by fish in temperate marine environments. Limnol. Oceanogr. 64, 2755–2770. https://doi.org/10.1002/lno.11339.
Sarmiento, J.L., 2006. Ocean Biogeochemical Dynamics. Princeton University Press. https://doi.org/10.1515/9781400849079.
Sarmiento, J.L., Murnane, R., Quere, C.L., Keeling, R., Williams, R.G., 1995. Air-sea CO_2 transfer and the carbon budget of the. Philos. Trans. R. Soc. B 348, 211–219. https://doi.org/10.1098/rstb.1995.0063.
Schauer, K.L., Grosell, M., 2017. Fractionation of the Gulf toadfish intestinal precipitate organic matrix reveals potential functions of individual proteins. Comp. Biochem. Physiol. A Mol. Integr. Physiol. 208, 35–45. https://doi.org/10.1016/j.cbpa.2017.03.007.
Schauer, K.L., LeMoine, C.M.R., Pelin, A., Corradi, N., McDonald, M.D., Warren, W.C., Grosell, M., 2016. A proteinaceous organic matrix regulates carbonate mineral production in the marine teleost intestine. Sci. Rep. 6, 34494 https://doi.org/10.1038/srep34494.
Schauer, K.L., Christensen, E.A.F., Grosell, M., 2018. Comparison of the organic matrix found in intestinal $CaCO_3$ precipitates produced by several marine teleost species. Comp. Biochem. Physiol. A Mol. Integr. Physiol. 221, 15–23. https://doi.org/10.1016/j.cbpa.2018.03.007.
Schiebel, R., 2002. Planktic foraminiferal sedimentation and the marine calcite budget. Glob. Biogeochem. Cycles 16. https://doi.org/10.1029/2001GB001459, 3-1-3–21.
Siegel, D.A., Buesseler, K.O., Behrenfeld, M.J., Benitez-Nelson, C.R., Boss, E., Brzezinski, M.A., Burd, A., Carlson, C.A., D'Asaro, E.A., Doney, S.C., Perry, M.J., Stanley, R.H.R., Steinberg, D.K., 2016. Prediction of the export and fate of Global Ocean net primary production: the EXPORTS science plan. Front. Mar. Sci. 3 https://doi.org/10.3389/fmars.2016.00022.
Sjöberg, E.L., Rickard, D.T., 1984. Temperature dependence of calcite dissolution kinetics between 1 and 62 °C at pH 2.7 to 8.4 in aqueous solutions. Geochim. Cosmochim. Acta 48, 485–493. https://doi.org/10.1016/0016-7037(84)90276-X.
Stanley, S.M., Hardie, L.A., 1998. Secular oscillations in the carbonate mineralogy of reef-building and sediment-producing organisms driven by tectonically forced shifts in seawater chemistry. Palaeogeogr. Palaeoclimatol. Palaeoecol. 144, 3–19. https://doi.org/10.1016/S0031-0182(98)00109-6.
Stieglitz, J.D., Hoenig, R.H., Baggett, J.K., Tudela, C.E., Mathur, S.K., Benetti, D.D., 2021. Advancing production of marine fish in the United States: olive flounder, *Paralichthys olivaceus*, aquaculture. J. World Aquacult. Soc. 52, 566–581. https://doi.org/10.1111/jwas.12804.
Stieglitz, J.D., Hoenig, R.H., Tudela, C.E., Mathur, S.K., Anchieta Da Silva, L., Ibarra-Castro, L., Benetti, D.D., 2022. Advancing sustainable marine fish production for the southeast U.S. and Caribbean: Advancements in yellowtail snapper, *Ocyurus chrysurus*. World Aquaculture Society Annual Meeting, San Diego, CA, US.

Subhas, A.V., Dong, S., Naviaux, J.D., Rollins, N.E., Ziveri, P., Gray, W., Rae, J.W.B., Liu, X., Byrne, R.H., Chen, S., Moore, C., Martell-Bonet, L., Steiner, Z., Antler, G., Hu, H., Lunstrum, A., Hou, Y., Kemnitz, N., Stutsman, J., Pallacks, S., Dugenne, M., Quay, P.D., Berelson, W.M., Adkins, J.F., 2022. Shallow calcium carbonate cycling in the North Pacific Ocean. Glob. Biogeochem. Cycles 36, e2022GB007388. https://doi.org/10.1029/2022GB007388.

Sulpis, O., Jeansson, E., Dinauer, A., Lauvset, S.K., Middelburg, J.J., 2021. Calcium carbonate dissolution patterns in the ocean. Nat. Geosci. 14, 423–428. https://doi.org/10.1038/s41561-021-00743-y.

Tamburini, C., Garcin, J., Grégori, G., Leblanc, K., Rimmelin, P., Kirchman, D., 2006. Pressure effects on surface Mediterranean prokaryotes and biogenic silica dissolution during a diatom sinking experiment. Aquat. Microb. Ecol. 43, 267–276. https://doi.org/10.3354/ame043267.

Tamburini, C., Goutx, M., Guigue, C., Garel, M., Lefèvre, D., Charrière, B., Sempéré, R., Pepa, S., Peterson, M.L., Wakeham, S., Lee, C., 2009. Effects of hydrostatic pressure on microbial alteration of sinking fecal pellets. Deep-Sea Res. II Top. Stud. Oceanogr. 56, 1533–1546. https://doi.org/10.1016/j.dsr2.2008.12.035.

Volk, T., Hoffert, M.I., 2013. Ocean carbon pumps: Analysis of relative strengths and efficiencies in ocean-driven atmospheric CO_2 changes. In: Sundquist, E.T., Broecker, W.S. (Eds.), Geophysical Monograph Series. American Geophysical Union, Washington, D. C, pp. 99–110. https://doi.org/10.1029/GM032p0099.

Walsh, P.J., Blackwelder, P., Gill, K.A., Danulat, E., Mommsen, T.P., 1991. Carbonate deposits in marine fish intestines: a new source of biomineralization. Limnol. Oceanogr. 36, 1227–1232. https://doi.org/10.4319/lo.1991.36.6.1227.

Ware, J.R., Smith, S.V., Reaka-Kudla, M.L., 1992. Coral reefs: sources or sinks of atmospheric CO_2? Coral Reefs 11, 127–130. https://doi.org/10.1007/BF00255465.

Wentworth, C.K., 1922. A scale of grade and class terms for clastic sediments. J. Geol. 30, 377–392. https://doi.org/10.1086/622910.

Whittamore, J.M., Cooper, C.A., Wilson, R.W., 2010. HCO_3^- secretion and $CaCO_3$ precipitation play major roles in intestinal water absorption in marine teleost fish in vivo. Am. J. Phys. Regul. Integr. Comp. Phys. 298, R877–R886. https://doi.org/10.1152/ajpregu.00545.2009.

Wilson, R.W., Grosell, M., 2003. Intestinal bicarbonate secretion in marine teleost fish—source of bicarbonate, pH sensitivity, and consequences for whole animal acid–base and calcium homeostasis. Biochim. Biophys. Acta Biomembr. 1618, 163–174. https://doi.org/10.1016/j.bbamem.2003.09.014.

Wilson, R.W., Gilmour, K.M., Henry, R.P., Wood, C.M., 1996. Intestinal base excretion in the seawater-adapted rainbow trout: a role in acid-base balance? J. Exp. Biol. 199, 2331–2343.

Wilson, R.W., Wilson, J.M., Grosell, M., 2002. Intestinal bicarbonate secretion by marine teleost fish—why and how? Biochimica et Biophysica Acta (BBA) - Biomembranes 1566, 182–193. doi:https://doi.org/10.1016/S0005-2736(02)00600-4.

Wilson, R.W., Millero, F.J., Taylor, J.R., Walsh, P.J., Christensen, V., Jennings, S., Grosell, M., 2009. Contribution of fish to the marine inorganic carbon cycle. Science 323, 359–362. https://doi.org/10.1126/science.1157972.

Woosley, R.J., Millero, F.J., Grosell, M., 2012. The solubility of fish-produced high magnesium calcite in seawater. J. Geophys. Res. 117, C04018 https://doi.org/10.1029/2011JC007599.

Zeebe, R.E., 2012. History of seawater carbonate chemistry, atmospheric CO_2, and ocean acidification. Annu. Rev. Earth Planet. Sci. 40, 141–165. https://doi.org/10.1146/annurev-earth-042711-105521.

Zheng, L., Yapa, P.D., 2000. Buoyant velocity of spherical and nonspherical bubbles/droplets. J. Hydraul. Eng. 126, 852–854. https://doi.org/10.1061/(ASCE)0733-9429(2000)126:11(852).